



Newly identified roles for PIEZO1 mechanosensor in controlling normal megakaryocyte development and in primary myelofibrosis

Vittorio Abbonante^{1,2} | Anastasia Iris Karkempetzaki^{3,4} | Catherine Leon⁵ | Anandi Krishnan⁶ | Nasi Huang³ | Christian A. Di Buduo¹ | Daniele Cattaneo⁷ | Christina Marie Ward³ | Shinobu Matsuura³ | Ines Guinard⁵ | Josiane Weber⁵ | Aurora De Acutis⁸ | Giovanni Vozzi⁸ | Alessandra Iurlo⁷  | Katya Ravid³ | Alessandra Balduini^{1,9} 

¹Department of Molecular Medicine, University of Pavia, Pavia, Italy

²Department of Health Sciences, Magna Graecia University of Catanzaro, Catanzaro, Italy

³Department of Medicine and Whitaker Cardiovascular Institute, Boston University Chobanian & Avedisian School of Medicine, Boston, Massachusetts, USA

⁴School of Medicine, University of Crete, Heraklion, Greece

⁵INSERM, EFS Grand Est, BPPS UMR-S 1255, Université de Strasbourg, Strasbourg, France

⁶Institute of Immunology, Stanford University School of Medicine, Palo Alto, California, United States

⁷Hematology Division, Foundation IRCCS Ca' Granda Ospedale Maggiore Policlinico, Milan, Italy

⁸Interdepartmental Research Center "E. Piaggio", University of Pisa, Pisa, Italy

⁹Department of Biomedical Engineering, Tufts University, Medford, Massachusetts, USA

Correspondence

Katya Ravid, Department of Medicine and Whitaker Cardiovascular Institute, Boston University Chobanian & Avedisian School of Medicine, Boston, MA, USA.
Email: kravid@bu.edu

Alessandra Balduini, Department of Molecular Medicine, University of Pavia, Pavia, Italy.
Email: alessandra.balduini@unipv.it

Funding information

Agence Nationale de la Recherche, Grant/Award Number: ANR-18-CE14-0037; Associazione Italiana per la Ricerca sul Cancro, Grant/Award Number: AIRC IG 2016 18700; Ministero della Salute, Grant/Award Number: GR-2016-02363136; Ministero dell'Istruzione, dell'Università e della Ricerca, Grant/Award Number: PRIN 2017-Z5LR5Z; National Heart, Lung, and Blood Institute, Grant/Award Numbers: HL158670, T32 HL007224, T32 HL007501; National Institutes of Health, Grant/Award Numbers:

Abstract

Mechanisms through which mature megakaryocytes (Mks) and their progenitors sense the bone marrow extracellular matrix to promote lineage differentiation in health and disease are still partially understood. We found PIEZO1, a mechanosensitive cation channel, to be expressed in mouse and human Mks. Human mutations in *PIEZO1* have been described to be associated with blood cell disorders. Yet, a role for PIEZO1 in megakaryopoiesis and proplatelet formation has never been investigated. Here, we show that activation of PIEZO1 increases the number of immature Mks in mice, while the number of mature Mks and Mk ploidy level are reduced. Piezo1/2 knockout mice show an increase in Mk size and platelet count, both at basal state and upon marrow regeneration. Similarly, in human samples, PIEZO1 is expressed during megakaryopoiesis. Its activation reduces Mk size, ploidy, maturation, and proplatelet extension. Resulting effects of PIEZO1 activation on Mks resemble the profile in Primary Myelofibrosis (PMF). Intriguingly, Mks derived from *Jak2*^{V617F} PMF mice show significantly elevated PIEZO1 expression, compared to wild-type controls.

Vittorio Abbonante, Anastasia Iris Karkempetzaki, Katya Ravid, and Alessandra Balduini contributed equally to this study.

This is an open access article under the terms of the [Creative Commons Attribution](https://creativecommons.org/licenses/by/4.0/) License, which permits use, distribution and reproduction in any medium, provided the original work is properly cited.

© 2024 The Authors. *American Journal of Hematology* published by Wiley Periodicals LLC.

1K08HG010061-01A1, 3UL1TR001085-04S1,
NIH OD/ORIP SERCA K01 OD025290

Accordingly, Mks isolated from bone marrow aspirates of *JAK2*^{V617F} PMF patients show increased PIEZO1 expression compared to Essential Thrombocythemia. Most importantly, PIEZO1 expression in bone marrow Mks is inversely correlated with patient platelet count. The ploidy, maturation, and proplatelet formation of Mks from *JAK2*^{V617F} PMF patients are rescued upon PIEZO1 inhibition. Together, our data suggest that PIEZO1 places a brake on Mk maturation and platelet formation in physiology, and its upregulation in PMF Mks might contribute to aggravating some hallmarks of the disease.

1 | INTRODUCTION

Megakaryocytes (Mks), the platelet progenitors, differentiate from hemopoietic stem cells within bone marrow under the control of thrombopoietin (TPO). Besides soluble stimuli, physical cues such as extracellular matrix (ECM) architecture, composition, and mechanical stimulation also contribute to Mk differentiation and function. Previous studies, including our own, demonstrated that Mks cultured on soft substrates exhibit enhanced maturation and platelet production compared to stiffer substrates.^{1–7} However, the underlying mechanisms through which Mks sense and respond to the bone marrow environment, and how it influences their differentiation, remain poorly understood in both healthy and diseased conditions.

Cellular mechanosensitive ion channels play key roles in interpreting extracellular information, translating it into intracellular signals that impact various biological processes, including blood cell functions.⁸ We previously showed that Mks express the Transient Receptor Potential Vanilloid 4 cation channel, which gets activated by soft substrates and promotes platelet formation.⁵ PIEZO1 is another cation channel that senses mechanical forces acting on the lipid plasma membrane and influences cell fate transitions and tissue homeostasis in multiple tissues.^{9–12} Loss-of-function mutations lead to an autosomal recessive form of lymphatic malformation 6 (LMPHM6; 616843),¹³ while gain-of-function PIEZO1 mutations are associated with autosomal dominant Dehydrated Hereditary Stomatocytosis (DHS1; 194380), a syndrome characterized by hemolytic anemia.¹⁴ PIEZO1 is expressed by erythrocytes and following mechanical activation controls their hydration status.¹⁵ Interestingly, PIEZO1 has also been implicated in platelet function.^{16–18} Studies have shown that shear stress or the agonist Yoda1 activates PIEZO1 in platelets and Meg-01 cell line, while the peptide inhibitor GsMTx4 attenuates calcium (Ca²⁺) influx.¹⁶ The presence of PIEZO1 in platelets implicates its potential role earlier during Mk development, and potentially also in platelet biogenesis. This could be particularly relevant in the context of diseases associated with a stiff ECM as PIEZO1 expression and function are increased in diseases with altered tissue stiffness, such as fibrotic conditions.^{9,19}

Chromosome Philadelphia-negative Myeloproliferative Neoplasms (MPN) are a group of clonal hematological neoplasia originating from hemopoietic stem cells. They comprise three clinically distinct disorders: Polycythemia Vera, Essential thrombocythemia (ET), and Primary Myelofibrosis (PMF), characterized by a fibrotic, stiff marrow.

MPNs share common driver mutations affecting the *MPL*, the *CALR*, and most commonly the *JAK2* gene (*JAK2*^{V617F}).^{20–22} PMF hallmarks are megakaryocytosis, with atypical immature Mks, and the accumulation of cross-linked collagen and reticulin fibers in the bone marrow, which gradually alter ECM architecture and stiffness.^{23–26} With the progression of the disease, PMF patients often present with thrombocytopenia, and high fibrosis grade, which are indicative of a more advanced disease state.²⁷ In vitro, Mks derived from PMF patients recapitulate most of the alterations found in vivo, including reduced maturation and proplatelet formation.^{28–30}

In this study, we present novel findings demonstrating the expression and function of the mechanosensitive cation channel PIEZO1 in mouse and human Mks. Pharmacological modulation of PIEZO1 in culture or genetic knockout in vivo was found to impact Mk and platelet development under normal conditions and in the context of PMF. These results expand our understanding of the repertoire of mechanosensors involved in the regulation of megakaryopoiesis.

2 | MATERIALS AND METHODS

2.1 | Transgenic mouse models

JAK2^{V617F} mice, constitutively expressing the Vav1-hJAK2V617F transgene carrying the human JAK2V617F mutation (generous gift of Dr. Zhizhuang Joe Zhao from University of Oklahoma)³¹ were backcrossed with C57BL/6J (Jackson laboratory), brought to homozygosity and used within at least 10 generations. Age- and sex-matched C57BL/6J wild-type mice served as controls.

The floxed *Piezo1* (*Piezo1*^{tm2.1.Apat/J}, # 029213) and *Piezo2* (B6(SLJ)-*Piezo2*^{tm2.2.Apat/J}, # 027720) mice were obtained from the Jackson Laboratory. Positive founder mice were bred and cross-bred with C57BL/6-Tg(Pf4-icre)Q3Rsko/J mice (denoted as Pf4Cre^{+/+}) from Jackson laboratory (#008535) to obtain mice with inactivation of both *Piezo1* and *Piezo2* in the MK lineage (named hereafter *Piezo1/2* DKO mice). Pf4Cre^{+/+} transgenic mice express a codon-improved Cre recombinase (iCre) under the control of the mouse platelet factor 4 (Pf4) gene promoter.^{32,33} RT-PCR was performed to confirm exons deletion in *Piezo1* mRNA (forward primer 5'CCTTCTGTTGCTGGTGTGTTGAG3' and reverse primer 5'AGCGTGAGGAACAGACAGTAG3') and *Piezo2* (forward primer 5'CGTGCTGATGTTTCTGGCTG3' and reverse primer

5'GAAGATGACCTTGCCAGCT3'). All mouse work was performed under a Boston University Institutional Animal Care and Use Committee-approved protocol and agreement for experimentation was obtained from the French government (N°15336-2018060110203508).

2.2 | Primary mouse bone marrow culture and small compound treatments

Bone marrow was flushed from the femurs and tibias of either control or transgenic mice as previously described.³⁴ Cells were cultured in Iscove's modified Dulbecco's medium (Gibco, cat# 21056-23) supplemented with 10% heat-inactivated fetal bovine serum, 100 units/mL of penicillin and 100 ug/ml of streptomycin (Gibco, cat# 15140-122), 200 mM GlutaMAX (Gibco, cat# 35050-061), and 25 ng/mL of TPO (PEG-MGDF, gift of Kirin Brewery, Japan). PIEZO1 agonist, Yoda-1 (Tocris, cat# 5586) was solubilized in dimethyl sulfoxide (DMSO). Under these culturing conditions (for 3–5 days) bone marrow cells develop and provide an ECM composed of lawn of cells, such as fibroblasts and mesenchymal stem cells, as well as matrix proteins released by the cells. The short spider venom peptide GsMTx4 (Smartox Biotechnology, cat#1209500-46-08) was solubilized in water and used fresh for each experiment. For experiments conducted with Yoda-1 and GsMTx4, 2–6 μ M concentrations were delivered to each bone marrow culture at the start of culture (Day 0). Control wells were set up to receive equal volume concentrations of DMSO as vehicle control, typically at a 10^3 dilution. Cultures were maintained at 37°C in a tissue culture incubator at 95% O₂/5% CO₂ for 4–5 days before being used in downstream applications.

2.3 | Mouse bone marrow Lineage-negative cells (Lin⁻) sorting for 3D culture in methylcellulose hydrogel

Mk differentiation in liquid or 3D hydrogel culture was performed as described.³⁵ Briefly, cells recovered from femurs and tibias using the mouse hematopoietic progenitor (Lin⁻) cell enrichment kit (Stem Cell Technologies, cat# 19856) were encapsulated in 2% methylcellulose (MC) gel (R&D systems, cat# HSC001) at room temperature at a concentration of 1×10^6 cells/mL in the presence of TPO (50 ng/mL) (Stem Cell Technologies, cat# 78210), hirudin (100 U/mL, Transgene) and 10% fetal calf serum (FCS). After 4 days in culture, cells were recovered by gel dilution in phosphate-buffered saline (PBS), and mature Mks were isolated by a bovine serum albumin (BSA) density gradient as previously described.³⁶

2.4 | Isolation of Mks from mouse bone marrow cultures

Mks derived from bone marrow cultures of either control or transgenic mice were isolated by a BSA density gradient.³⁶ Briefly, a 1.5% w/v solution of BSA was layered onto 3% w/v solution of BSA dissolved in Dulbecco's phosphate-buffered saline (DPBS) in a conical tube. Bone marrow cultures were suspended in serum-free media and

layered at top of the gradient. After 30 min, cells that settled at the bottom of the tube were collected and rinsed twice with pre-warmed 37°C DPBS before the start of all downstream applications.

2.5 | Human Mk culture

Human cord blood (CB) was collected from the local CB bank following healthy pregnancies and deliveries with the informed consent of the parents. All samples were processed following the ethical committee of the Istituto di Ricovero e Cura a Carattere Scientifico (IRCCS) Policlinico San Matteo Foundation and the principles of the Helsinki Declaration. Human peripheral blood samples were obtained from healthy donor controls and patients with MPNs after informed consent. CD34⁺ hematopoietic progenitor cells were separated by immunomagnetic bead selection (Miltenyi Biotec, cat# 130-046-702) and differentiated in Stem Span medium (STEMCELL Technologies Inc. cat# 09650), as previously described.³⁷

2.6 | Patients

This study was approved by the Foundation IRCCS Ca' Granda Ospedale Maggiore Policlinico, Milan, Italy, and the Foundation IRCCS Policlinico San Matteo, Pavia, Italy. The procedures followed were in accordance with the Helsinki Declaration of 1975 (revised 2000). Samples were obtained after written informed consent. Diagnosis of MPN was made according to the 2016 revision of the World Health Organization classification of myeloid neoplasms.²⁰ Genetic mutations were studied as previously described.³⁸ Patient characteristics are given in Tables S1, S2. For platelet RNA-seq, study approval was provided by the Stanford University Institutional Review Board (#18329). We collected blood from MPN patients enrolled in the Stanford University and Stanford Cancer Institute Hematology Tissue Bank between December 2017 and 2020 after written informed consent from patients or their legally authorized representative. Eligibility criteria included age \geq 18 years and Stanford MPN clinic diagnosis of essential thrombocythemia or myelofibrosis (defined using the consensus criteria at the time of this study). For healthy controls, blood was collected from adult donors selected at random from the Stanford Blood Center. All donors were requested consent for genetic research. Together, our platelet transcriptome data set³⁹ comprised 87 human peripheral blood samples as follows: healthy donor controls ($n = 21$) and World Health Organization-defined MPN patients (24 ET and 42 MF) either untreated, or on cytoreductives/biologics (e.g., ruxolitinib, hydroxyurea, interferon-alpha), anti-thrombotic agents (e.g., aspirin, warfarin), or a combination reflecting the real-life diversity among MPN patients.

2.7 | mRNA extraction, quantitative real-time PCR, and in situ hybridization

BSA gradient-purified primary mouse Mks were lysed and homogenized using QIASHredder columns (Qiagen, cat# 79656). For

experiments where bone marrow cultures were derived from individual mice, the RNeasy micro kit (Qiagen, cat#74034) was used for RNA extraction. The RNeasy mini kit (Qiagen, cat# 74034) was used for mRNA isolation from bone marrow cultures obtained from pooled samples. QuantiTect Reverse transcription reaction kit was used for cDNA synthesis (Qiagen, cat # 205311). Quantitative Real-time PCR was performed with the following TaqMan gene expression primers and probes purchased from Applied Biosystems; Piezo1 (Applied Biosystems, cat# 4331192), Piezo2 (Applied Biosystems, cat# 4331182), and 18s rRNA (Applied Biosystems, cat# 4319413E). Samples were run on an Applied biosystems Via7ii (Thermo Fisher Scientific). Data was normalized to the housekeeping gene 18S rRNA. For experiments conducted with bone marrow that was cultured from individual mice the data was analyzed using the Δ CT, and data from pooled cultures data was analyzed with the $\Delta\Delta$ CT method.

Reverse transcription on human Mks was performed in a final volume of a 20- μ L reaction using the iScriptTM cDNA Synthesis Kit (Bio-Rad, cat# 1708891) according to the manufacturer's instructions. Pre-designated KiCqStartTM primers for human PIEZO1 were purchased from Sigma-Aldrich (cat# KSPQ12012G). Samples were loaded on a 2% agarose gel containing ethidium bromide and visualized with a ChemiDoc XRS Imaging System (Bio-Rad). Transcribed samples were diluted up to three times with ddH₂O and the resulting cDNA was amplified in triplicate with 200 nM of each primer and SsoFast EvaGreen Supermix (Bio-Rad, cat# 1725201). The amplification was performed in a CFX real-time system (Bio-Rad, USA).

In situ hybridization assay carried out on mouse Mks was performed with the RNAscope technology (Bio-Techne) using a mix of 20 probes targeting the *mus musculus* Piezo1 mRNA (Bio-Techne cat# 400181).

2.8 | Flow cytometry assay

For analysis by flow cytometry, cells from mouse primary bone marrow cultures were collected on culture Day 4. Each sample was rinsed twice with ice-cold PBS. All samples were assessed for viability with live-dead staining using a 1:200 dilution of Aqua Zombie (BioLegend, cat# 423102) and incubated for 15 min at room temperature. To integrate the number of Mks present in each culture, samples were rinsed in ice-cold PBS then re-suspended in staining buffer (PBS with 2 mM EDTA, 0.5% BSA) containing a 1:200 dilution of phycoerythrin (PE) conjugated anti-CD41 antibody (eBioscience, cat# 12-0411-83) and a 1:200 dilution of allophycocyanin (APC) conjugated anti-CD42 antibody (Invitrogen, cat# 17042182). In order to determine the expression of PIEZO1 on Mks, each sample was first stained with a 1:100 dilution of anti-Piezo1 antibody (Proteintech, cat# 15939-1-AP) for 1 h on ice followed by staining with PE conjugated anti-mouse Ab (anti-rabbit Alexa flour 594 secondary) secondary antibody. Then samples were stained with a 1:200 dilution of APC conjugated anti-CD41 antibody. All samples were run on a LSRII flow cytometer (BD Bioscience) and data was

collected using FACs Diva software and analyzed with FlowJo version 10.

To analyze ploidy state of Mks from primary bone marrow cultures, cells were collected on culture Day 4, rinsed in DPBS, and fixed in ice-cold fresh 70% ethanol. Samples were stained for 15 min at room temperature with a 1:200 dilution of FITC conjugated anti-CD41 antibody (BD Bioscience, cat# 553848). Samples were then rinsed and resuspended in staining buffer. Just prior to analysis, propidium iodide and RNase were added to each tube at a final concentration of 0.05 and 0.1 mg/mL, respectively. Samples were run on a LSRII flow cytometer (BD Bioscience), data were collected using FACs Diva software, and data were analyzed with FlowJo version 10.8.1 from BD Biosciences. Events were gated around FITC CD41⁺ cells and then analyzed for DNA content.

Human Mk maturation was analyzed using FITC anti-human CD41 (Beckman Coulter, clone SZ22) and PE anti-human CD42b (Beckman Coulter, clone SZ2). For human Mk ploidy, cells were fixed overnight in ice-cold 70% ethanol at -20°C . Sample were incubated in PBS with 100 $\mu\text{g}/\text{mL}$ of RNase and propidium iodide solution and stained with 5 μL of FITC anti-human CD41. All samples were acquired with a Beckman Coulter Navios flow cytometer. Non-stained samples, FITC, and PE-isotype controls were used to set the correct analytical gating. Off-line data analysis was performed using Beckman Coulter Kaluza analysis software.

2.9 | Western blotting

Cord blood-derived human Mks were lysed for 30 min at 4°C in HEPES-glycerol lysis buffer (50 mM HEPES, pH 7.4, 150 mM NaCl, 10% glycerol, 1% Triton X-100 [Sigma Aldrich, cat# T9284], 1.5 mM MgCl₂, 1 mM EGTA) containing 1 $\mu\text{g}/\text{mL}$ leupeptin (Sigma Aldrich, cat# L2884) and 1 $\mu\text{g}/\text{mL}$ aprotinin (Sigma Aldrich, cat# A1153). Samples were clarified by centrifugation at 15 700 \times g at 4°C for 15 min. Laemmli sample buffer was then added to supernatants. Samples were heated at 95°C for 3 min, separated by electrophoresis on 3–8% CriterionTM XT Tris-Acetate (Bio-Rad, cat# 3450129), and then transferred to polyvinylidene fluoride membranes (Bio-Rad, cat# 1620177). Membranes were probed with primary antibodies, washed three times with PBS (Sigma Aldrich, cat# P4417) and Tween 0.1% (Bio-Rad, cat# 1610781), and incubated with peroxidase-conjugate secondary antibodies. Membranes were visualized using Immobilon western chemiluminescent horseradish peroxidase (HRP) substrate (Millipore, cat# WBKLS0), images were acquired by UVITEC Alliance Mini HD9 (UVitec, U.K.), and the protein levels detected were quantified using UVITEC NineAlliance 1D software.

Primary bone marrow Mks were isolated from MPN patients by means of CD61 positive immunomagnetic-bead selection (Miltenyi Biotec, cat# 130-051-101). Mk purity was evaluated by CD42b staining and flow cytometry analysis. Samples with a Mk purity $>85\%$ were lysed. Mk lysates from MPN patients were analyzed with an automated capillary-based immunoassay platform (Wes, ProteinSimple), according to the manufacturer instructions. Briefly, Mk lysates were diluted to the required

concentration with sample buffer, then prepared by adding master mix containing 200 mM dithiothreitol, sample buffer, and fluorescent standards (Standard Pack 1, cat# PS-ST01-8) and boiled for 5 min at 95°C. Wes 66–440 kDa prefilled microplates were used (cat# SM-W008). Compass Software for Simple Western was used to analyze results (version 3.1.7, ProteinSimple). Separation time was set to 25 min, stacking loading time to 15 s, and sample loading time to 9 s. Primary antibodies were incubated for 30 min and the High Dynamic Range (HDR) profile was used for detection. For each antibody, a lysate dilution experiment was performed first to confirm the optimal dynamic range of the corresponding protein on Wes. This was followed by an antibody optimization experiment to compare a range of dilutions and to select an antibody concentration that was close to saturation level to allow a quantitative comparison of signals between samples.⁴⁰

2.10 | Immunofluorescence

For immunofluorescence microscopy assays, mature human Mks (1×10^5) were plated to adhere onto fibronectin-coated (Corning, cat# 10526961) glass coverslips for the indicated time. For intracellular staining, adhering Mks were washed with PBS, fixed in 4% paraformaldehyde (PFA) for 20 min, permeabilized with 0.1% Triton X-100 for 5 min, and stained for immunofluorescence evaluation with anti-PIEZO1 (Proteintech, cat# 15939-AP) and anti- β 1-tubulin (Abcam, cat# ab179511) as previously described.⁴⁰ The coverslips were mounted onto glass slides with ProLong Gold antifade reagent (Invitrogen, cat# P10144). Images were acquired with a confocal laser-scanning microscope Olympus Fluoview FV10i (Olympus, Tokyo, Japan).

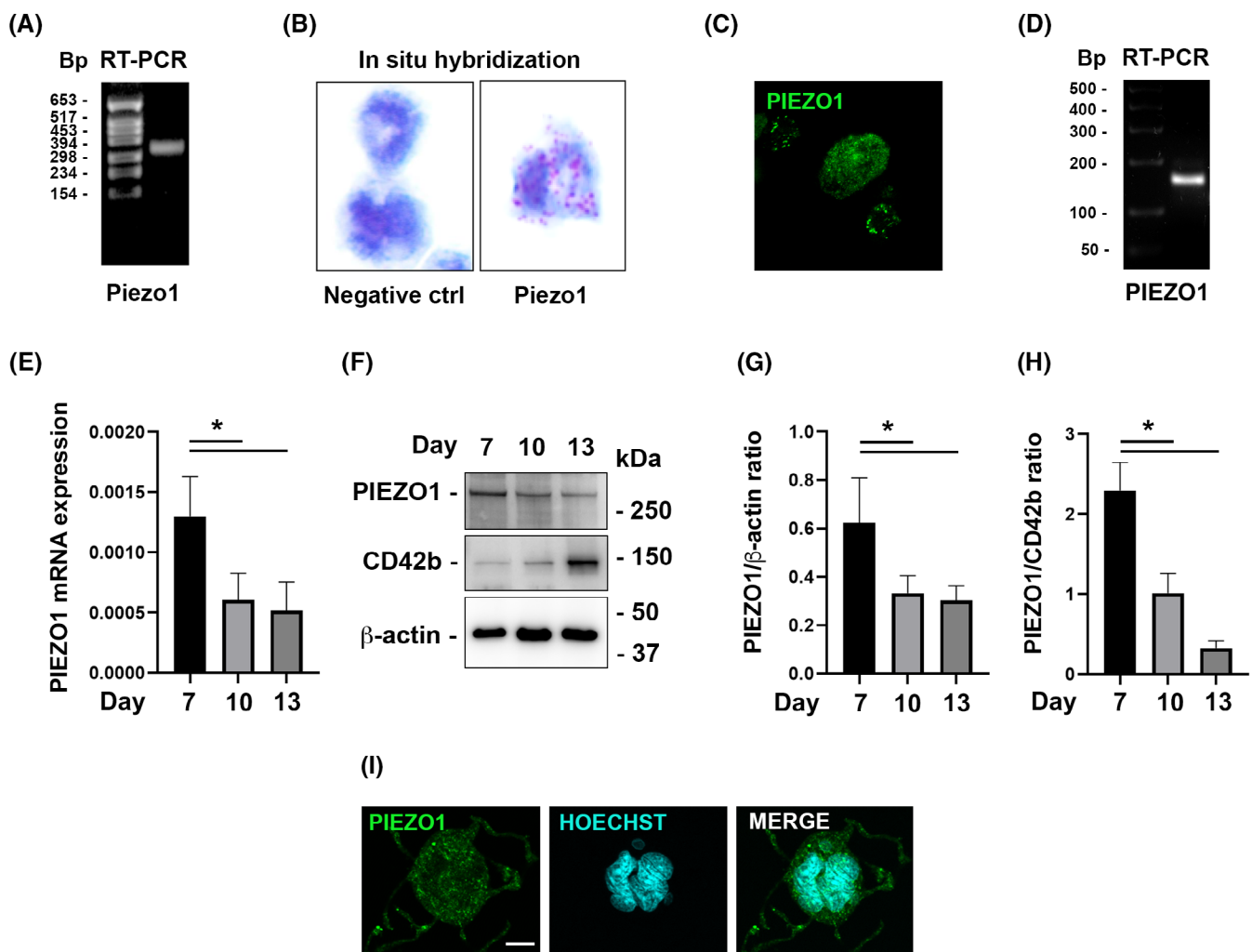


FIGURE 1 PIEZO1 is expressed in mouse and human megakaryocytes (Mks). (A) RT-PCR analysis of *Piezo1* gene expression performed on mRNA from the mouse Mk culture. (B) PIEZO1 in situ hybridization showing its expression in fully mature MKs, revealed by red dots. (C) Representative immuno-staining image (40 \times) of gradient-purified cultured Mks (see Section 2) derived from 12-week-old wild-type mice and stained with anti-Piezo1, showing punctate peripheral staining in medium-size Mks, and diffused more dim staining in large ones. (D) RT-PCR analysis of *PIEZO1* gene expression in human Mks. (E) qRT-PCR analysis of *PIEZO1* gene expression by human Mks during differentiation, $n = 3$. (F–H) Western blot analysis of PIEZO1 protein expression by human Mks during differentiation, $n = 3$. (I) Immunofluorescence staining of PIEZO1 protein (green) in human Mks. Nuclei were counterstained with HOECHST. Scale bar is 10 μ m. Data are expressed as mean \pm standard deviation. * $p < 0.05$. [Color figure can be viewed at wileyonlinelibrary.com]

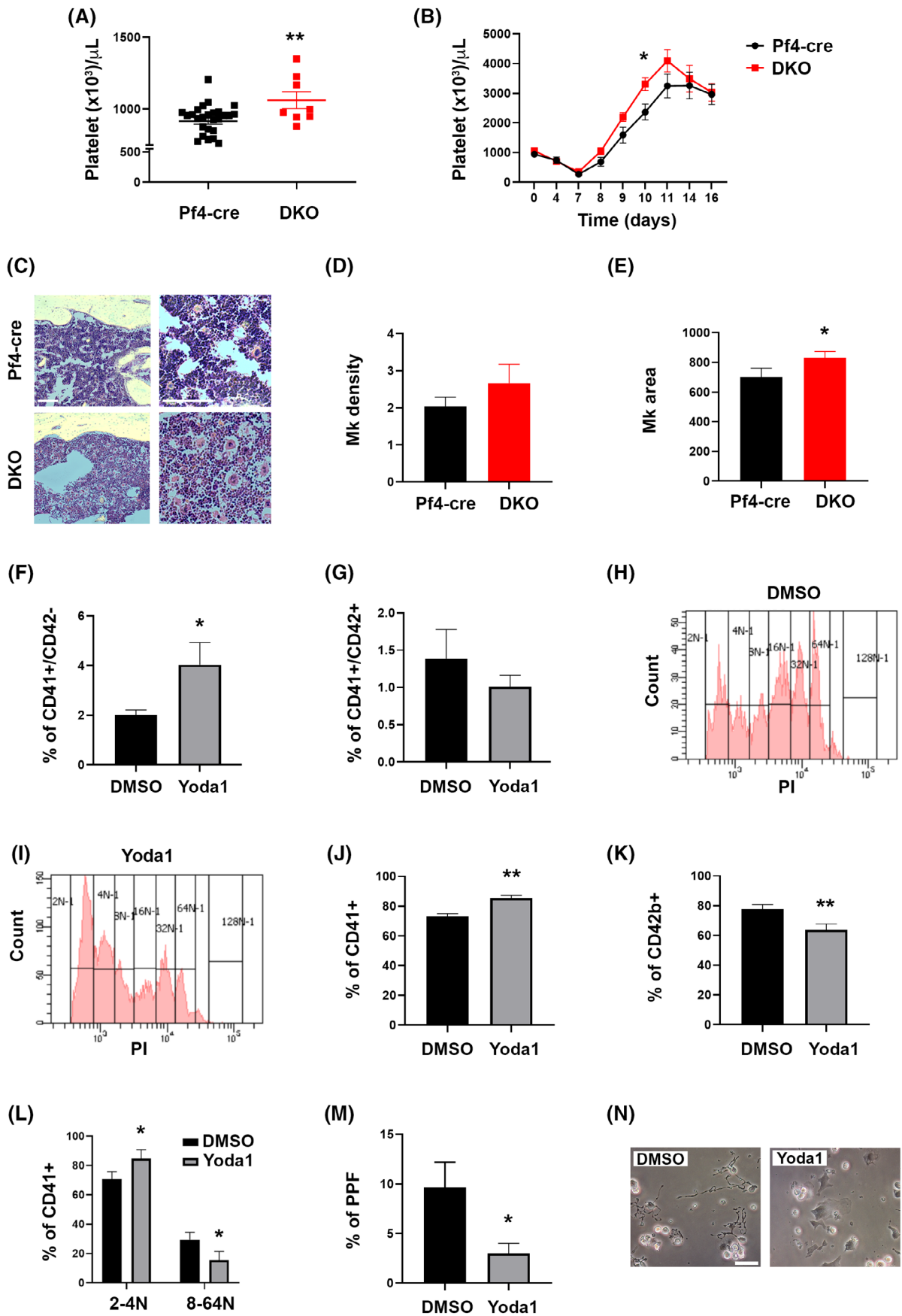


FIGURE 2 Legend on next page.

2.11 | Mouse circulating platelet measurement

Mice were anesthetized with isoflurane and maintained at 38°C. The tail extremity was cut (<0.5 mm) and a drop of 10 µL blood recovered in EDTA anticoagulant (6 mM). Cell count was obtained using a veterinary hematology counter (Element HT5—Scil veterinary excellence). In some experiments, mice were injected i.p. with 150 mg/kg 5-fluorouracil (5-FU) and the kinetic of platelet loss and recovery followed during the following 2 weeks.

2.12 | Human platelet isolation, library preparation, and RNA sequencing

All blood samples were collected into acid citrate-dextrose (ACD, 3.2%) sterile tubes (Becton, Dickinson and Co.) and platelets were isolated with an established protocol^{41–44} within 4 h of collection. For RNA-sequencing (RNA-seq), 1×10^9 isolated platelets lysed in TRIzol were processed to extract RNA (all integrity numbers > 7.0) and library preparation. Twelve pooled samples with individual indices were run on an Illumina HiSeq 4000 (Patterned flow cell with HiSeq 4000 SBS v3 chemistry, Illumina, Inc.) as 2×75 bp paired end sequencing with a coverage target of 40 M reads/sample.

2.13 | Fabrication of 3D silk fibroin-based scaffolds

Silk fibroin aqueous solution was obtained from *Bombyx mori*, as previously described.⁵ Dewormed cocoons were boiled in Na₂CO₃ solution, and the dried fibers were solubilized in LiBr to obtain 8% or 16% w/v silk fibroin solutions. The solutions were mixed with Type A gelatin and sterile alginate acid in the presence of ions and glucose, at pH 7.4. The formulations were then mixed with human Mks and dispensed into a well-plate by a BIO-X extrusion bioprinter (CELLINK). The printing process was performed with cylindrical steel needles. After deposition, the 3D scaffold has been cross-linked with CaCl₂ and cultured in classic culture medium, as described above.

2.14 | Mechanical test

Mechanical tests were carried out in a universal testing machine at a crosshead speed of 10% h0/min (h0 is the sample's thickness). A cylindrical flat-faced plunger with a diameter of 50 mm and a load cell of 10 N were used. Experiments were performed up to achieving a deformation of 20% of h0 in each sample, respectively.

2.15 | Statistical analysis

The data are reported as the mean ± standard deviation from at least three replicates from independent experiments or per individual mice. A 2-tailed Student's *t*-test was used for comparisons between two groups. For comparisons of 1 factor across multiple groups, one-way ANOVA was performed followed by the post-hoc Tukey test. Platelet transcriptomic data were library-size-corrected, variance-stabilized, and log₂-transformed using the R package DESeq2,⁴⁵ and normalized gene expression determined for PIEZO1. For downstream analyses comparing any two groups, a parametric two-tailed unpaired student *t*-test was used. Summary statistics were used to describe the study cohort and clinical variables were expressed as the mean ± error of the mean or as a number and percentage (%). GraphPad Prism 8 (GraphPad Software) was used for statistical analysis and graphing. Values of *p* < 0.05 were considered statistically significant.

3 | RESULTS

3.1 | Mouse and human Mks express PIEZO1

Mouse Mks were tested for the expression of the mechanosensitive cation channel PIEZO1. RT-PCR showed clear expression of PIEZO1 in cultured Mks (Figure 1A). Presence of PIEZO1 in individual mature Mks was confirmed by in situ hybridization (Figure 1B) and further validated at the protein level through immunostaining (Figure 1C). The expression of PIEZO1 was also confirmed in in vitro-derived human

FIGURE 2 PIEZO1 activation impairs megakaryocyte maturation and proplatelet formation. (A) Mouse platelet count in DKO mice compared to Pf4-Cre control mice; data are expressed as mean ± standard error of the mean (sem), *n* = 28 for Pf4-Cre control mice, 8 for DKO mice. (B) Platelet kinetic recovery following 5-fluorouracil intraperitoneal administration at day 0 (150 mg/kg); data are expressed as mean ± sem, *n* = 8 mice. (C) Representative hematoxylin and eosin staining of bone marrow sections from Pf4-Cre and DKO mice. Scale bar is 200 µm. (D) Number of Mks per square surface unit (5000 µm²) of bone marrow. Data are expressed as mean ± standard deviation (SD), *n* = 3. (E) Area of Mks expressed in µm². Data are expressed as mean ± SD, *n* = 3. (F, G) Percentages of CD41 + CD42- and CD41 + CD42+ mouse Mks on day 4 of dimethyl sulfoxide (DMSO; vehicle) or 4 µM Yoda1-treated bone marrow cultures were determined by flow cytometry. Cells were derived from 8- to 16-week-old female C57BL/6J control mice. At least four experiments were performed, and three mice were used per group in each experiment. Data are expressed as mean ± SD. (H, I) Representative ploidy profiles of Mks derived as in panels (F, G) and treated with vehicle (DMSO) or 4 µM Yoda1 (see also Figure S2). (J–N) Human CB-derived CD34⁺ cells were differentiated to Mks in presence or not of 3 µM of the PIEZO1 pharmacological agonist Yoda1. DMSO was used as vehicle control. Data are expressed as mean ± SD, *n* = 4 DMSO, and *n* = 4 Yoda1. (J, K) Flow cytometry analysis of the early Mk marker CD41 and the late Mk marker CD42b at the end of the culture. (L) Flow cytometry analysis of low ploidy (2–4 N) and high ploidy (8–64 N) CD41⁺ Mks. (M) Proplatelet formation assay. Mks extending proplatelets were counted and expressed as the percentage of adhered Mks with or without proplatelet extensions. A minimum of 40 Mks per sample was analyzed. (N) Representative image of Mks extending proplatelets. Scale bar is 100 µm. **p* < 0.05; ***p* < 0.01. [Color figure can be viewed at wileyonlinelibrary.com]

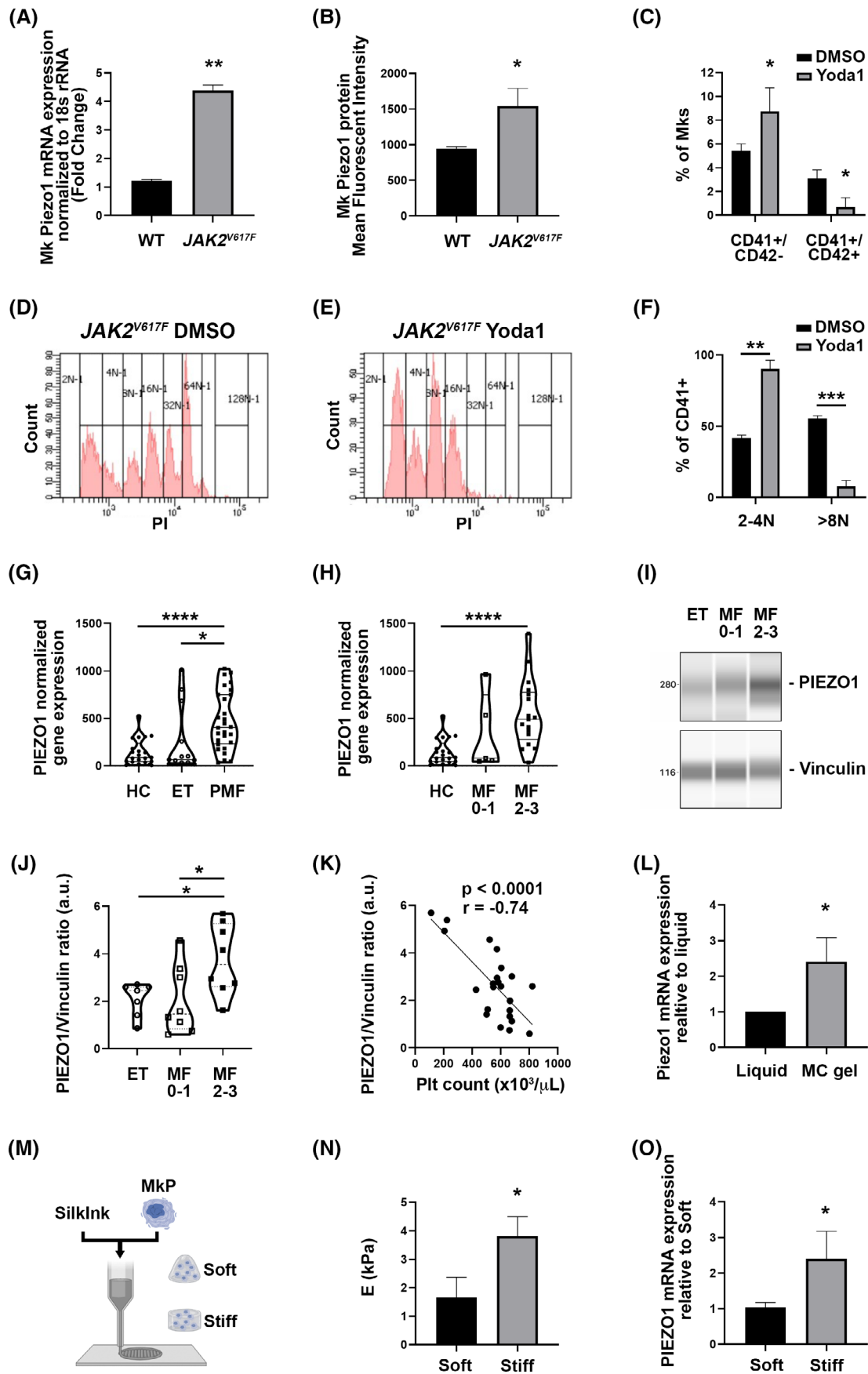


FIGURE 3 Legend on next page.

Mks, both at mRNA and protein levels (Figure 1D–I). Of note, the expression of PIEZO1 decreases during Mk maturation (Figure 1E,H).

3.2 | PIEZO1 negatively controls platelet level and proplatelet formation by impairing Mk maturation

To study the role of PIEZO1 in megakaryopoiesis, we generated mice deleted of *Piezo1* and *Piezo2* genes in the Mk lineage (DKO mice) (Figure S1) by cross-breeding floxed mice with mice expressing Cre recombinase under the control of the Pf4 promoter.³³ Although we found the expression of mouse *Piezo2* mRNA to be minute (hardly detectable by qRT-PCR) compared to *Piezo1* (data not shown), to mitigate a possible compensatory effect of *Piezo2*, we focused on DKO. DKO mice presented a slightly though significantly increased number of circulating platelets (Figure 2A). Under conditions of acute myeloid leukemia/myeloregeneration induced by 5-FU challenge, we observed the persistence of a significantly higher number of circulating platelets in DKO mice (Figure 2B), thus suggesting that activation of PIEZO channels may restrain platelet production. Analysis of bone marrow sections showed a slightly though not significantly increased number of Mks, which appeared to increase in size in DKO mice, compared to controls (Figure 2C–E).

To gain further insight into the role of PIEZO1 in the regulation of megakaryopoiesis, we treated mouse bone marrow cells with the PIEZO1 pharmacological agonist Yoda1, a small molecule which acts as a gating modifier by specifically binding PIEZO1, and lowering the mechanical threshold for its activation.^{15,46} Culturing mouse bone marrow cells in presence of Yoda1 resulted in a significant increase in CD41⁺CD42⁻ cells (less mature Mks) and a tendency for a decrease in the number of CD41⁺CD42⁺ cells (mature Mks) (Figure 2F,G). There was also a significant shift to lower Mk ploidy upon PIEZO1 activation (Figure 2H,I and Figure S2).

The effect of PIEZO1 activation on Mk differentiation and function was also tested using human samples. The differentiation of human cord-blood-derived CD34⁺ progenitors in presence of Yoda1 treatment resulted in a statistically significant reduction of Mk maturation as demonstrated by the increase in the percentage of CD41⁺ Mks and a significant reduction in the percentage of more mature CD42b⁺ Mks (Figure 2J,K), as also supported by a shift toward lower Mk ploidy (Figure 2L). To evaluate the functional consequences of the reduced Mk maturation, we studied proplatelet formation. Mks differentiated in presence of Yoda1 showed a significant reduction in proplatelet formation (Figure 2M,N).

3.3 | PIEZO1 is upregulated in *JAK2*^{V617F} myelofibrotic mice and patients

Myelofibrosis is a pathological condition that strongly modifies the mechanical properties of the bone marrow. We thus evaluated PIEZO1 in *JAK2*^{V617F} mice that reproduce the human pathology. Interestingly, qRT-PCR as well as flow cytometric assay showed an increased expression of PIEZO1 at mRNA and protein levels in Mks derived from *JAK2*^{V617F} mice, compared to matching controls (Figure 3A,B). In this case too, activation with Yoda1 resulted in a significant increase in CD41⁺CD42⁻ cells and a decrease in the number of CD41⁺CD42⁺ cells (mature Mks) (Figure 3C). PIEZO1 activation also led to a sharp shift to a low Mk ploidy level (Figure 3D–F). Using the GsMTx4 inhibitor at different concentrations and up to 5 μM (to avoid cell death) tended to shift Mk number to mature ones, but it was not statistically significant (data not shown).

The analysis of a large cohort of MPN patients demonstrated the upregulation of PIEZO1 expression in platelets from PMF patients compared to ET patients and healthy donor controls (Figure 3G). Furthermore, PIEZO1 expression was higher in platelets isolated from

FIGURE 3 PIEZO1 expression is increased in a primary myelofibrosis (PMF) mouse model and in patients affected by *JAK2*^{V617F} PMF. (A) Mk *Piezo1* mRNA was determined by qRT-PCR in isolated Mks from cultured bone marrow cells derived from 12- to 16-week-old male and female *JAK2*^{V617F} ($n = 8$) and matching controls ($n = 9$). Data are expressed as mean \pm standard deviation (SD). (B) *Piezo1* cell surface expression was determined by staining bone marrow cultures derived from matching control and *JAK2*^{V617F} male mice with CD41⁺ and *Piezo1* antibody. Data shown are the mean fluorescent intensity \pm SD, $n = 3$. (C) Percentages of CD41⁺CD42⁻ and CD41⁺CD42⁺ Mks on Day 4 of DMSO- (vehicle) or 4 μM Yoda1-treated bone marrow cultures were determined by flow cytometry. Cells were derived from 8- to 16-week-old female or male *JAK2*^{V617F} mice. At least four experiments were performed, and three mice were used per group in each experiment. Data are expressed as mean \pm SD. (D, E) Representative ploidy profiles of Mks derived as in panels (C, D) and treated with vehicle (DMSO; left panel) or 4 μM Yoda1 (right panel). (F) Quantification of the percentage of CD41⁺ mouse Mks with lower (2–4 N) and higher (>8 N) ploidy derived as in panels (C, D) and treated with vehicle (DMSO) or 4 μM Yoda1. (G) PIEZO1-normalized platelet gene expression in healthy controls (HC), ET, and PMF patients. (H) PIEZO1 normalized platelet gene expression in HC, early PMF (fibrosis grade 0–1), and overt PMF (fibrosis grade 2–3) patients. (I) Mks were isolated from bone marrow aspirates derived from patients affected by ET and PMF. PIEZO1 protein expression was analyzed by quantitative capillary-based electrophoresis with anti-PIEZO1 antibody. Anti-vinculin antibody was used for loading control. Representative data are shown as blots. (J) Peak areas were quantified and expressed as the ratio of PIEZO1/vinculin. (K) Correlation (r) between PIEZO1 protein expression in bone marrow Mks and peripheral blood platelet count. (L) qRT-PCR analysis of *Piezo1* gene expression in mouse Mks grown in 3D gel compared to liquid culture. Data are expressed as mean \pm standard error of the mean normalized to liquid culture, $n = 3$. (M) Human Mks were cultured in 3D bone marrow-like tissues having different mechanical features. (N) Elastic modulus of fibroin silk-based 3D bone marrow-like tissues. Data are expressed as mean \pm SD, $n = 4$. (O) qRT-PCR analysis of *PIEZO1* gene expression in human Mks cultured in the 3D bone marrow-like tissues having different mechanical features. Data are expressed as mean \pm SD, $n = 3$. * $p < 0.05$; ** $p < 0.01$; *** $p < 0.001$; **** $p < 0.0001$. [Color figure can be viewed at wileyonlinelibrary.com]

patients affected by overt PMF (fibrosis grade 2–3) compared to early PMF (fibrosis grade 0–1) (Figure 3H).

Similarly, we measured PIEZO1 expression in Mks isolated from bone marrow aspirates derived from MPN patients affected by PMF or ET (Table S1). PIEZO1 expression was significantly higher in bone marrow Mks isolated from patients affected by overt PMF compared to early PMF and ET. (Figure 3I,J). Furthermore, the expression of PIEZO1 in bone marrow Mks negatively correlated with peripheral

blood platelet count (Figure 3K), thus suggesting a role for PIEZO1 as a negative regulator of platelet production.

To evaluate whether the typical alterations in the mechanical features of the fibrotic bone marrow might be responsible for the increased PIEZO1 expression,²⁵ we cultured mouse and human Mks in different 3D microenvironments (Figure 3L–O). First, we used an in vitro model of 3D confinement by growing mouse Mks in a physical hydrogel of MC and comparing them with Mks grown in liquid

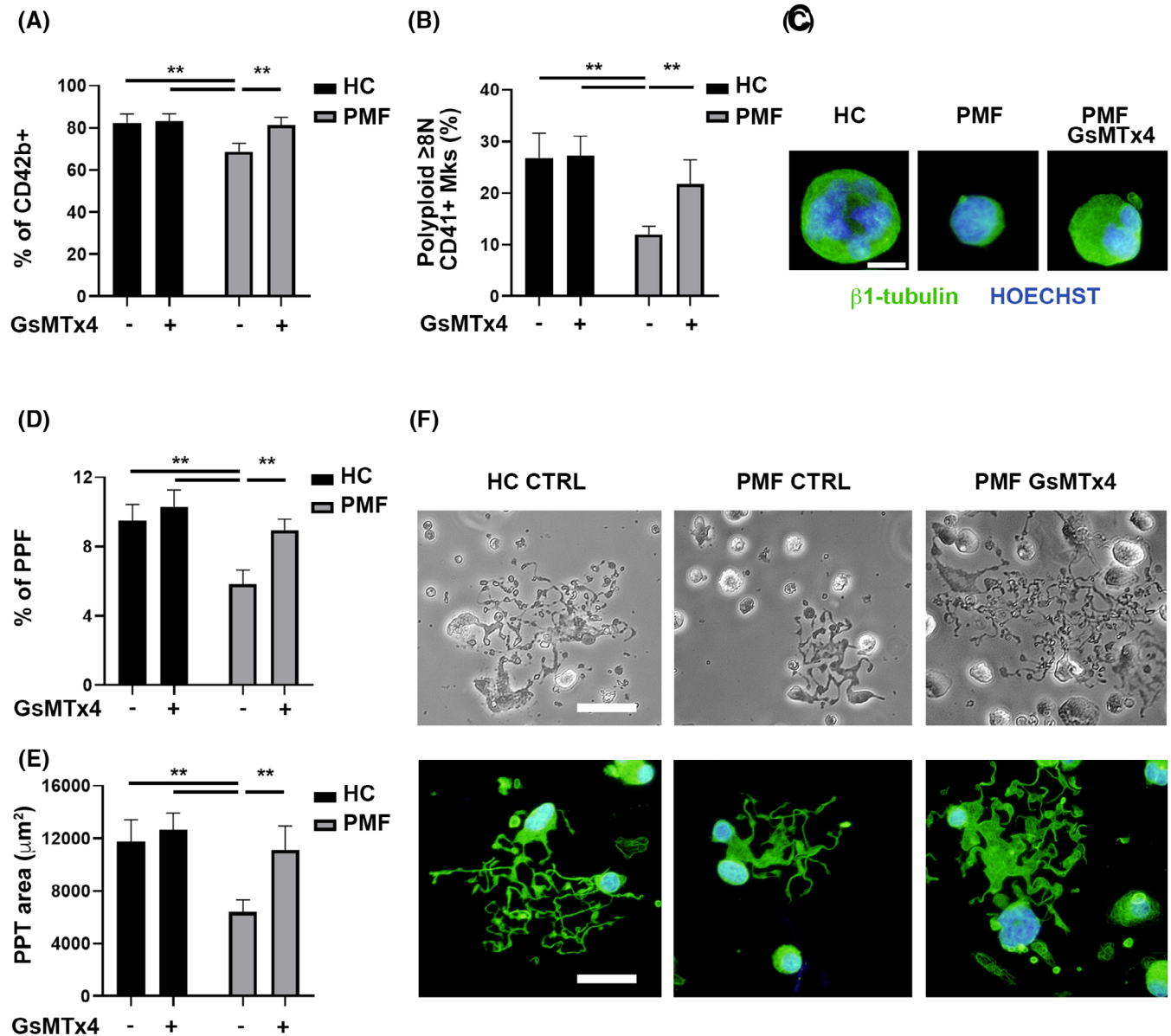


FIGURE 4 PIEZO1 inhibition increases megakaryocyte (Mk) maturation and proplatelet formation of *JAK2*^{V617F} primary myelofibrosis (PMF) Mks. CD34+ progenitors derived from healthy controls (HC, *n* = 5) and patients affected by *JAK2*^{V617F} primary myelofibrosis (PMF, *n* = 5) were differentiated in Mks in presence or not of 5 μM of the PIEZO1 inhibitor GsMTx4. (A) Flow cytometry analysis of CD42b + Mks at the end of the culture. (B) Flow cytometry analysis of the ploidy of CD41 + Mks. (C) Representative immunofluorescence images of HC and PMF Mks stained with anti-β1-tubulin (green). Nuclei were counterstained with HOECHST. Scale bar is 20 μm. Where indicated, PMF Mks were differentiated in the presence of 5 μM GsMTx4. (D) Proplatelet formation (PPF) assay. Mks extending proplatelets were counted and expressed as the percentage of adhered Mks. A minimum of 40 Mks per sample was analyzed. (E) The proplatelet (PPT) area was calculated. (F) Representative phase contrast and immunofluorescence microscopy images of proplatelet extending Mks. Scale bar is 100 μm. Data are expressed as mean ± SD **p* < 0.05; ***p* < 0.01. [Color figure can be viewed at wileyonlinelibrary.com]

medium.⁴ We found Piezo1 to be overexpressed in the 3D culture compared to classic liquid culture (Figure 3L). Then, we took advantage of silk fibroin biomaterial to fabricate 3D bone marrow-like tissues having different mechanical features (Figure 3M–O). Human Mk grown into the stiff microenvironment demonstrated increased expression of PIEZO1, when compared to the soft 3D matrix (Figure 3O). This strongly suggested that the PIEZO1 overexpression in overt PMF patients may result from alterations of marrow stiffness/confinement.

3.4 | Rescue of some cellular hallmarks of PMF in the presence of PIEZO1 inhibitor

We studied whether PIEZO1 inhibition *in vitro* might rescue the typical defects in maturation and proplatelet formation found in PMF Mk.^{28–30} Mk were differentiated from CD34⁺ progenitors derived from thrombocytopenic *JAK2*^{V617F} overt PMF patients (Table S2) and from healthy donor controls. A higher percentage of mature CD42b⁺ Mk was obtained when PMF Mk were differentiated in the presence of 5 μM GsMTx4, a PIEZO1 inhibitor acting as a gating modifier^{47,48} (Figure 4A and Figure S3). The increase in Mk maturation was further confirmed by ploidy analysis, showing a significant increase in polyploid (≥8 N) Mk (Figure 4B,C and Figure S3). The rise in Mk maturation was associated with an increase in proplatelet formation (Figure 4D–F). We previously demonstrated that *in vitro* cultured PMF Mk extend a reduced number of small proplatelet when compared to healthy donor control-derived Mk.²⁸ Differentiation of PMF Mk in presence of GsMTx4 rescued both the percentage of proplatelet forming Mk and the branching area of proplatelets to a level nearly comparable to healthy donor control-derived Mk (Figure 4D–F).

4 | DISCUSSION

Recent studies highlighted the crucial role of the ECM mechanical properties within the bone marrow microenvironment in various aspects of Mk development, including lineage commitment, polyploidization, and proplatelet formation.^{1,5,7,49} Overall, the differentiation, maturation, and proplatelet formation are favored when Mk sense a softer environment. However, the specific plasma membrane sensors in Mk that mediate the effects of the ECM have yet to be fully elucidated. In our study, we unveil the involvement of the mechanosensor PIEZO1 in the regulation of Mk maturation and proplatelet biogenesis under normal physiological conditions. Moreover, we observed elevated expression levels of PIEZO1 in Mk derived from both mice and patients affected by *JAK2*^{V617F} PMF, a condition characterized by a stiff ECM. This upregulation of PIEZO1 expression may contribute to the pathological megakaryopoiesis observed in PMF and the reduced platelet production observed in advanced stages of the disease. Different mutation types may determine the characteristics of the disease leading to alterations in Piezo1 expression. This aspect could be

explored further in the future, particularly in the context of various MPN driver mutations. We observed that PIEZO1 is expressed early in Mk development during normal megakaryopoiesis, but its expression decreases during terminal maturation. This suggests that PIEZO1 plays a specific physiological role in the early phases of Mk maturation. Supporting this hypothesis, we found that pharmacological activation of PIEZO1 in Mk progenitors hampers Mk maturation and polyploidization, and their ability to extend proplatelets. To further confirm the involvement of PIEZO1 in the regulation of megakaryopoiesis and platelet production, we generated mice with a specific deletion of *Piezo1/2* in the megakaryocytic lineage. Our unpublished preliminary studies showed that in normal Mk the expression of mouse *Piezo2* is at least 10-fold lower than that of *Piezo1*. Still, we resorted to double knockout mice to exclude any potential compensatory mechanism of *Piezo2*. In these mice, we observed an increase in Mk size and peripheral blood platelet count both under basal conditions and after 5-FU challenge. Taken together, our data indicates that PIEZO1 acts as a brake on fully mature Mk differentiation *in vitro* and proper platelet production *in vitro* and *in vivo*. Interestingly, this role appears to be shared by both Mk and erythroid progenitors. A recent study also showed a higher expression of PIEZO1 in early erythroid progenitors followed by a decrease during terminal maturation. In these cells, PIEZO1 activation by either chemical or gain-of-function mutations delayed erythrocyte differentiation,¹¹ similar to our observations in the Mk lineage.

Reduced Mk differentiation is a hallmark of PMF, a clonal hematological neoplasia characterized by profound alterations of the bone marrow microenvironment due to the progressive accumulation of a stiff ECM constituted of reticulin and collagen fibers.^{25,50,51} These atypical Mk and the ECM alterations are not found in the bone marrow of patients affected by ET, a MPN subtype characterized by high platelet count.⁵¹ We observed elevated expression levels of PIEZO1 protein in Mk isolated from the bone marrow of both mice and patients affected by *JAK2*^{V617F} PMF. Furthermore, our analysis demonstrated that PIEZO1 expression in Mk increases in advanced fibrotic PMF patients (grade 2–3). These findings were further supported by analysis of the platelet transcriptome from a large cohort of PMF patients, ET patients, and healthy controls. Our analysis confirmed that PIEZO1 protein expression is higher in PMF patients compared to ET patients and healthy controls, and this higher expression level is characteristic of advanced fibrotic PMF patients. All these data suggested that PIEZO1 might play a role in the pathogenesis of PMF and that the altered bone marrow mechanical properties might upregulate PIEZO1 expression. Accordingly, we tested this contention using cultured cells, since previous studies demonstrated that the typical defects of Mk maturation found in PMF patients, including polyploidization and proplatelet formation, are maintained *in vitro*.^{28,30} Our results demonstrated that PIEZO1 pharmacological inhibition partially rescued the aberrant Mk phenotype associated with PMF. This finding suggests that the inhibition of PIEZO1 activity holds potential as a therapeutic strategy to mitigate the pathological effects observed in Mk development in PMF patients.

The excessive accumulation of ECM in fibrotic microenvironment, combined with increased matrix crosslinking by lysyl oxidase,²⁴ inevitably leads to deregulated mechanical properties, such as under stiffness.^{52,53} In these scenarios, PIEZO1 has been shown to have a pivotal role through a feed-forward circuit, where the stiffer microenvironment upregulates the expression and activation of the channel, leading to pro-fibrotic responses.^{54,55} Recently, higher bone marrow stiffness has also been shown in *JAK2^{V617F}* mouse model of PMF.^{25,26} Accordingly, a suggested correlation between PIEZO1 expression and the mechanical characteristics of the bone marrow in PMF is further supported by our experiments using 3D in vitro models that mimic the stiffness of fibrotic bone marrow, which resulted in increased PIEZO1 expression in cultured Mks. In our ex-vivo culture systems, changes in ECM elicited by cells bearing the *JAK2^{V617F}* mutation, whether through augmented release of Mk lysyl oxidase or fibronectin or inflammatory factors,^{40,56–59} are likely to contribute to differential responses of Mk Piezo activation in the control versus mutated condition.

PIEZO1 is known to play a crucial role in transducing externally applied forces at the plasma membrane, and aberrant mechanical micro-environments might negatively affect cells through this channel.^{60–62} In the present study, we found an inverse correlation between the expression level of PIEZO1 protein, measured in bone marrow Mks, and peripheral blood platelet counts, suggesting that high expression of the channel negatively impacts platelet biogenesis. In addition, the central role of PIEZO1 as a driver of a mechanothrombotic pathway has been demonstrated in different scenarios such as diabetes and hypertension.^{17,18} Future studies will determine whether the increased PIEZO1 expression observed in platelets from PMF patients might contribute to increased thrombotic risk that is described in these patients.^{63,64}

In conclusion, our study highlights the involvement of the mechanosensor PIEZO1 in regulating Mk maturation and proplatelet biogenesis. The upregulation of PIEZO1 in PMF suggests its potential contribution to the aberrant megakaryopoiesis observed in this disease. These findings underscore the significance of ECM sensors in modulating Mk function and platelet production, providing a foundation for future investigations aimed at developing targeted therapies for Mk and/or platelet disorders associated with altered mechanosensing pathways.

ACKNOWLEDGMENTS

We thank Dr. Carla Mazzeo and Dr. Aikaterini Karagianni for assistance with immunostaining and qRT-PCR. We thank the group of Carlo Gaetano (Fondazione Maugeri, Pavia, Italy) for helping with Wes, ProteinSimple analysis. We thank Dr. Jason Gotlib at Stanford University, the MPN patients at the Stanford Cancer Institute, and the healthy donors at the Stanford Blood Center for their contribution to this research. Ines Guinard and this work were supported by the French ANR (Agence Nationale de la Recherche) Grant ANR-18-CE14-0037.

FUNDING INFORMATION

Mouse-related research was supported by NHLB grant to KR (HL158670) and Grant ANR PlatForMechanics-18-CE14-0037 to

CL. Other funding includes the Associazione Italiana per la Ricerca sul Cancro (AIRC IG 2016 18700), Italian Ministry of University and Research (PRIN 2017-Z5LR5Z), and EIC Transition Project SILKink (Project no. 101113073) to AB; Italian Ministry of Health (Ricerca Finalizzata Giovani Ricercatori GR-2016-02363136) to VA; US National Institutes of Health grant (1K08HG010061-01A1 and 3UL1TR001085-04S1) and the MPN Research Foundation Challenge Grant to AK. CMW was supported by NIH NHLBI Research Training grants in Biology and Research in Blood Diseases and Resources (T32 HL007501) and Multidisciplinary Training in Cardiovascular Research (T32 HL007224). SM was supported by NIH OD/ORIP SERCA K01 OD025290.

CONFLICT OF INTEREST STATEMENT

All authors have no conflicts of interest to declare that are relevant to the content of this article.

DATA AVAILABILITY STATEMENT

Data may be made available upon contact to the corresponding authors.

ORCID

Alessandra Iurlo  <https://orcid.org/0000-0002-4401-0812>

Alessandra Balduini  <https://orcid.org/0000-0003-3145-1245>

REFERENCES

- Shin JW, Swift J, Spinler KR, Discher DE. Myosin-II inhibition and soft 2D matrix maximize multinucleation and cellular projections typical of platelet-producing megakaryocytes. *Proc Natl Acad Sci USA*. 2011; 108(28):11458–11463.
- Pallotta I, Lovett M, Rice W, Kaplan DL, Balduini A. Bone marrow osteoblastic niche: a new model to study physiological regulation of megakaryopoiesis. *PLoS ONE*. 2009;4(12):e8359.
- Malara A, Gruppi C, Pallotta I, et al. Extracellular matrix structure and nano-mechanics determine megakaryocyte function. *Blood*. 2011; 118(16):4449–4453.
- Aguilar A, Pertuy F, Eckly A, et al. Importance of environmental stiffness for megakaryocyte differentiation and proplatelet formation. *Blood*. 2016;128:2022–2032.
- Abbonante V, Di Buduo CA, Gruppi C, et al. A new path to platelet production through matrix sensing. *Haematologica*. 2017;102(7): 1150–1160.
- Di Buduo CA, Wray LS, Tozzi L, et al. Programmable 3D silk bone marrow niche for platelet generation ex vivo and modeling of megakaryopoiesis pathologies. *Blood*. 2015;125(14):2254–2264.
- Guinard I, Nguyen T, Brassard-Jollive N, et al. Matrix stiffness controls megakaryocyte adhesion, fibronectin fibrillogenesis and proplatelet formation through Itgβ3. *Blood Adv*. 2023;7:4003–4018.
- Martinac B. Mechanosensitive ion channels: an evolutionary and scientific tour de force in mechanobiology. *Channels*. 2012;6(4):211–213.
- Chen X, Wanggou S, Bodalia A, et al. A feedforward mechanism mediated by mechanosensitive ion channel PIEZO1 and tissue mechanics promotes glioma aggression. *Neuron*. 2018;100(4):799–815.e797.
- Gudipaty SA, Lindblom J, Loftus PD, et al. Mechanical stretch triggers rapid epithelial cell division through Piezo1. *Nature*. 2017;543(7643): 118–121.
- Caulier A, Jankovsky N, Demont Y, et al. PIEZO1 activation delays erythroid differentiation of normal and hereditary xerocytosis-derived human progenitor cells. *Haematologica*. 2020;105(3):610–622.

12. Sugimoto A, Miyazaki A, Kawarabayashi K, et al. Piezo type mechanosensitive ion channel component 1 functions as a regulator of the cell fate determination of mesenchymal stem cells. *Sci Rep.* 2017;7(1):17696.
13. Lukacs V, Mathur J, Mao R, et al. Impaired PIEZO1 function in patients with a novel autosomal recessive congenital lymphatic dysplasia. *Nat Commun.* 2015;6:8329.
14. Andolfo I, Alper SL, De Franceschi L, et al. Multiple clinical forms of dehydrated hereditary stomatocytosis arise from mutations in PIEZO1. *Blood.* 2013;121(19):3925-3935.
15. Cahalan SM, Lukacs V, Ranade SS, Chien S, Bandell M, Patapoutian A. Piezo1 links mechanical forces to red blood cell volume. *Elife.* 2015;4:4.
16. Ilkan Z, Wright JR, Goodall AH, Gibbins JM, Jones CI, Mahaut-Smith MP. Evidence for shear-mediated Ca(2+) entry through mechanosensitive cation channels in human platelets and a megakaryocytic cell line. *J Biol Chem.* 2017;292(22):9204-9217.
17. Zhu W, Guo S, Homilius M, et al. PIEZO1 mediates a mechanothrombotic pathway in diabetes. *Sci Transl Med.* 2022;14(626):eabk1707.
18. Zhao W, Wei Z, Xin G, et al. Piezo1 initiates platelet hyperreactivity and accelerates thrombosis in hypertension. *J Thromb Haemost.* 2021;19(12):3113-3125.
19. Atcha H, Jairaman A, Holt JR, et al. Mechanically activated ion channel Piezo1 modulates macrophage polarization and stiffness sensing. *Nat Commun.* 2021;12(1):3256.
20. Arber DA, Orazi A, Hasserjian R, et al. The 2016 revision to the World Health Organization classification of myeloid neoplasms and acute leukemia. *Blood.* 2016;127(20):2391-2405.
21. Vainchenker W, Kralovics R. Genetic basis and molecular pathophysiology of classical myeloproliferative neoplasms. *Blood.* 2017;129(6):667-679.
22. Zoi K, Cross NC. Genomics of myeloproliferative neoplasms. *J Clin Oncol.* 2017;35(9):947-954.
23. Zahr AA, Salama ME, Carreau N, et al. Bone marrow fibrosis in myelofibrosis: pathogenesis, prognosis and targeted strategies. *Haematologica.* 2016;101(6):660-671.
24. Leiva O, Ng SK, Chitalia S, Balduini A, Matsuura S, Ravid K. The role of the extracellular matrix in primary myelofibrosis. *Blood Cancer J.* 2017;7(2):e525.
25. Vining KH, Marneth AE, Adu-Berchie K, et al. Mechanical checkpoint regulates monocyte differentiation in fibrotic niches. *Nat Mater.* 2022;21(8):939-950.
26. Leiva O, Ng SK, Matsuura S, et al. Novel lysyl oxidase inhibitors attenuate hallmarks of primary myelofibrosis in mice. *Int J Hematol.* 2019;110(6):699-708.
27. Benevolo G, Elli EM, Guglielmelli P, Ricco A, Maffioli M. Thrombocytopenia in patients with myelofibrosis: management options in the era of JAK inhibitor therapy. *Leuk Lymphoma.* 2020;61(7):1535-1547.
28. Balduini A, Badalucco S, Pugliano MT, et al. In vitro megakaryocyte differentiation and proplatelet formation in Ph-negative classical myeloproliferative neoplasms: distinct patterns in the different clinical phenotypes. *PLoS ONE.* 2011;6(6):e21015.
29. Ciurea SO, Merchant D, Mahmud N, et al. Pivotal contributions of megakaryocytes to the biology of idiopathic myelofibrosis. *Blood.* 2007;110(3):986-993.
30. Masselli E, Carubbi C, Gobbi G, et al. Protein kinase C ϵ inhibition restores megakaryocytic differentiation of hematopoietic progenitors from primary myelofibrosis patients. *Leukemia.* 2015;29(11):2192-2201.
31. Xing S, Wanting TH, Zhao W, et al. Transgenic expression of JAK2V617F causes myeloproliferative disorders in mice. *Blood.* 2008;111(10):5109-5117.
32. Tiedt R, Schomber T, Hao-Shen H, Skoda RC. Pf4-Cre transgenic mice allow the generation of lineage-restricted gene knockouts for studying megakaryocyte and platelet function in vivo. *Blood.* 2007;109(4):1503-1506.
33. Pertuy F, Aguilar A, Strassel C, et al. Broader expression of the mouse platelet factor 4-cre transgene beyond the megakaryocyte lineage. *J Thromb Haemost.* 2015;13(1):115-125.
34. Eliades A, Papadantonakis N, Bhatnagar A, et al. Control of megakaryocyte expansion and bone marrow fibrosis by lysyl oxidase. *J Biol Chem.* 2011;286(31):27630-27638.
35. Boscher J, Gachet C, Lanza F, Léon C. Megakaryocyte culture in 3D methylcellulose-based hydrogel to improve cell maturation and study the impact of stiffness and confinement. *J Vis Exp.* 2021;(174):e62511. doi:10.3791/62511
36. Drachman JG, Sabath DF, Fox NE, Kaushansky K. Thrombopoietin signal transduction in purified murine megakaryocytes. *Blood.* 1997;89(2):483-492.
37. Di Buduo CA, Abbonante V, Tozzi L, Kaplan DL, Balduini A. Three-dimensional tissue models for studying ex vivo megakaryocytopoiesis and platelet production. *Methods Mol Biol.* 2018;1812:177-193.
38. Rumi E, Pietra D, Ferretti V, et al. JAK2 or CALR mutation status defines subtypes of essential thrombocythemia with substantially different clinical course and outcomes. *Blood.* 2014;123(10):1544-1551.
39. Shen Z, Du W, Perkins C, et al. Platelet transcriptome identifies progressive markers and potential therapeutic targets in chronic myeloproliferative neoplasms. *Cell Rep Med.* 2021;2(10):100425.
40. Abbonante V, Malara A, Chrisam M, et al. Lack of COL6/collagen VI causes megakaryocyte dysfunction by impairing autophagy and inducing apoptosis. *Autophagy.* 2023;19(3):984-999.
41. Campbell RA, Franks Z, Bhatnagar A, et al. Granzyme a in human platelets regulates the synthesis of proinflammatory cytokines by monocytes in aging. *J Immunol.* 2018;200(1):295-304.
42. Rowley JW, Oler AJ, Tolley ND, et al. Genome-wide RNA-seq analysis of human and mouse platelet transcriptomes. *Blood.* 2011;118(14):e101-e111.
43. Middleton EA, Rowley JW, Campbell RA, et al. Sepsis alters the transcriptional and translational landscape of human and murine platelets. *Blood.* 2019;134(12):911-923.
44. Amisten S. A rapid and efficient platelet purification protocol for platelet gene expression studies. *Methods Mol Biol.* 2012;788:155-172.
45. Love MI, Huber W, Anders S. Moderated estimation of fold change and dispersion for RNA-seq data with DESeq2. *Genome Biol.* 2014;15(12):550.
46. Syeda R, Xu J, Dubin AE, et al. Chemical activation of the mechanotransduction channel Piezo1. *Elife.* 2015;4:4.
47. Gnanasambandam R, Ghatak C, Yasmann A, et al. GsMTx4: mechanism of inhibiting mechanosensitive ion channels. *Biophys J.* 2017;112(1):31-45.
48. Bae C, Sachs F, Gottlieb PA. The mechanosensitive ion channel Piezo1 is inhibited by the peptide GsMTx4. *Biochemistry.* 2011;50(29):6295-6300.
49. Choi JS, Harley BA. Marrow-inspired matrix cues rapidly affect early fate decisions of hematopoietic stem and progenitor cells. *Sci Adv.* 2017;3(1):e1600455.
50. Kuter DJ, Bain B, Mufti G, Bagg A, Hasserjian RP. Bone marrow fibrosis: pathophysiology and clinical significance of increased bone marrow stromal fibres. *Br J Haematol.* 2007;139(3):351-362.
51. Barbui T, Thiele J, Gisslinger H, et al. The 2016 WHO classification and diagnostic criteria for myeloproliferative neoplasms: document summary and in-depth discussion. *Blood Cancer J.* 2018;8(2):15.
52. Wells RG. Tissue mechanics and fibrosis. *Biochim Biophys Acta.* 2013;1832(7):884-890.
53. Piersma B, Hayward MK, Weaver VM. Fibrosis and cancer: a strained relationship. *Biochim Biophys Acta Rev Cancer.* 2020;1873(2):188356.
54. Zhao X, Kong Y, Liang B, et al. Mechanosensitive Piezo1 channels mediate renal fibrosis. *JCI Insight.* 2022;7(7):e152330.
55. Swain SM, Romac JM, Vigna SR, Liddle RA. Piezo1-mediated stellate cell activation causes pressure-induced pancreatic fibrosis in mice. *JCI Insight.* 2022;7(8):e158288.

56. Abbonante V, Di Buduo CA, Gruppi C, et al. Thrombopoietin/TGF- β 1 loop regulates megakaryocyte extracellular matrix component synthesis. *Stem Cells*. 2016;34(4):1123-1133.
57. Abbonante V, Chitalia V, Rosti V, et al. Upregulation of lysyl oxidase and adhesion to collagen of human megakaryocytes and platelets in primary myelofibrosis. *Blood*. 2017;130(6):829-831.
58. Malara A, Gruppi C, Abbonante V, et al. EDA fibronectin-TLR4 axis sustains megakaryocyte expansion and inflammation in bone marrow fibrosis. *J Exp Med*. 2019;216(3):587-604.
59. Malara A, Gruppi C, Rebuzzini P, et al. Megakaryocyte-matrix interaction within bone marrow: new roles for fibronectin and factor XIII-A. *Blood*. 2011;117(8):2476-2483.
60. Ridone P, Vassalli M, Martinac B. Piezo1 mechanosensitive channels: what are they and why are they important. *Biophys Rev*. 2019;11(5):795-805.
61. Nourse JL, Pathak MM. How cells channel their stress: interplay between Piezo1 and the cytoskeleton. *Semin Cell Dev Biol*. 2017;71:3-12.
62. Murthy SE, Dubin AE, Patapoutian A. Piezos thrive under pressure: mechanically activated ion channels in health and disease. *Nat Rev Mol Cell Biol*. 2017;18(12):771-783.
63. Barbui T, Carobbio A, Cervantes F, et al. Thrombosis in primary myelofibrosis: incidence and risk factors. *Blood*. 2010;115(4):778-782.
64. Barbui T, Ghirardi A, Carobbio A, et al. Increased risk of thrombosis in JAK2 V617F-positive patients with primary myelofibrosis and interaction of the mutation with the IPSS score. *Blood Cancer J*. 2022;12(11):156.

SUPPORTING INFORMATION

Additional supporting information can be found online in the Supporting Information section at the end of this article.

How to cite this article: Abbonante V, Karkempetzaki AI, Leon C, et al. Newly identified roles for PIEZO1 mechanosensor in controlling normal megakaryocyte development and in primary myelofibrosis. *Am J Hematol*. 2024;99(3):336-349. doi:[10.1002/ajh.27184](https://doi.org/10.1002/ajh.27184)